Electrochimica Acta 199 (2016) 59–69

Contents lists available at ScienceDirect

Electrochimica Acta

journal homepage: www.elsevier.com/locate/electacta

Effect of physical heterogeneity on the electromigration of nitrate in layered granular porous media

R.T. Gill[a,*], S.F. Thornton[a], M.J. Harbottle[b], J.W. Smith[a,c]

[a] Groundwater Protection & Restoration Group, University of Sheffield, Department of Civil & Structural Engineering, Kroto Research Institute, Broad Land, Sheffield S3 7HQ, UK
[b] Cardiff University, School of Engineering, Queen's Buildings, The Parade, Cardiff CF24 3AA, UK
[c] Shell Global Solutions, Lange Kleiweg 40, 2288 GK Rijswijk, The Netherlands

ARTICLE INFO

Article history:
Received 27 October 2015
Received in revised form 15 February 2016
Accepted 27 February 2016
Available online 15 March 2016

Keywords:
Electrokinetics
Bioremediation electromigration
Heterogeneity
Nitrate

ABSTRACT

The effect of physical heterogeneity on the electrokinetic (EK) transport of nitrate, an electron acceptor frequently used for anaerobic biodegradation, was investigated experimentally within saturated granular porous media comprising two layers of high and low hydraulic conductivity (K) material. Two hypotheses were tested: firstly, that the presence of layered physical heterogeneity will generate non-uniformities in the electric field; and secondly that this would create non-uniform electromigration of ions resulting in an additional nitrate flux into the lower-K layer. Experiments were conducted in bench-top test cells that contained electrode and sediment chambers. An aqueous nitrate solution (0, 0.1, 1 and 5 g-NO_3 L^{-1}) was added at the cathode and the experiments run with an idealised mixture of glass beads and kaolinite, and natural sediment and kaolinite. A constant current (1.6 A m^{-2}) was applied in all experiments. Results showed elevated voltage differences between layers in heterogeneous experiments compared to equivalent homogenous experiments. Furthermore, nitrate concentrations are elevated in the low-K material in heterogeneous compared with homogeneous systems. Using predicted values this is shown to be a function of a transverse flux associated with the voltage difference between layers. The importance of this phenomena at field scale for delivery of an amendment (i.e., electron acceptor, donor or nutrient) by EK for bioremediation is presented in an electron balance model. Overall, this research establishes and quantifies a previously unreported important phenomenon in the electrokinetic transport literature that enhance the application of this technology for bioremediation of contaminated aquifers.

1. Introduction

Aqueous phase contaminant plumes within physically heterogeneous aquifers (where hydraulic conductivity (K) varies) present a long-term management challenge. Contaminants can become sequestered in low-K zones within heterogeneous settings and persist as secondary sources of groundwater contamination. This occurs due to the presence of concentration gradients across the interface between a low-K zone and high-K host matrix that drives diffusion of contaminants into the low-K zone [1]. This concentration gradient is reversed after advection of contaminants from the high-K host matrix, resulting in back-diffusion of contaminants sequestered in the low-K zone into the host matrix over long timescales, which prolong remediation efforts [2] in situations where the mass flux relative to natural attenuation processes is sufficient to give rise to a site-specific risk. These scenarios are difficult to treat by conventional hydraulic-based techniques, such as pump and treat, due to this mass transfer limitation in low-K materials.

Electrokinetics (EK) is a technique that initiates solute transport phenomena independent of K, by applying direct current to porous media. EK processes comprise electromigration, electroosmosis and electrophoresis, which can be coupled with other technologies, such as bioremediation to enhance biodegradation of organic compounds *in situ*. At the micro-scale EK transport can increase mixing and improve contact between microorganisms, contaminants and nutrients to enhance bioaccessibility [3]; and at the macro-scale by increasing the supply of electron acceptors supporting biodegradation [4]. EK enhanced bioremediation (EK-BIO) is a potentially suitable technology to treat biodegradable compounds in physically heterogeneous settings, where EK can be used to overcome physical limitations on *in situ* biodegradation.

In advection-dominated systems there is limited flow across high- to low-K boundaries. Therefore, in physically heterogeneous settings bioremediation of low-K zones will be limited by the

* Corresponding author.
E-mail address: rich.gill87@gmail.com (R.T. Gill).

http://dx.doi.org/10.1016/j.electacta.2016.02.191

distribution and mixing of microbes and solutes [5]. In EK dominated systems physical heterogeneity is less inhibiting because the electric field is not directly affected by K. EK can be used to directly remove contaminants, such as lead and phenanthrene, from heterogeneous settings by electromigration and electroosmosis [6,7] and also introduce amendments within heterogeneous settings. For example, Reynolds et al. [8] migrated potassium permanganate into clay blocks within a high permeability host material to show the effectiveness of coupling EK with *in situ* chemical oxidation. However spatial changes in material type will still exert a control on solute migration by EK. Gill et al. [9] showed that the transition from high- to low-K porous media corresponds to a decrease in nitrate mass flux and increase in the voltage gradient. Both factors depend on the effective ionic mobility (EIM), itself a function of the porosity and tortuosity of a porous medium [10].

Electric fields in homogeneous 2-D settings can be non-uniform and create tortuous migration pathways for solute migration between electrodes [11]. Physical heterogeneity affects the arrangement of electric fields and will therefore create non-uniform flow paths relative to the distribution of high- and low-K zones [9]. These non-uniform flow paths are equivalent to fluxes and are important when trying to understand the efficacy of amendment delivery by EK in a remediation scenario.

The objectives of this study were to deduce the effect of EK transport on nitrate migration within homogeneous and heterogeneous settings, identify the controlling mechanisms for any differences observed and determine the influence of variations in nitrate concentration on amendment flux. Heterogeneity in this study is represented by two layers of granular porous media with different K values. The following hypotheses were tested:

1. A small voltage difference will exist between layers of material with different EIM values, due to the subsequent variation in ion mass flux into the sediment and effective electrical conductivity. Furthermore, this difference will increase with nitrate concentration;
2. This difference in voltage gradient will create an associated electromigration mass flux between layers and can be quantified by comparing nitrate transport in heterogeneous and homogeneous systems.

2. Materials and Methods

2.1. Material properties

The porous medium was created with two materials: soda-lime-silica glass beads (Potters Ballotini Ltd), to represent an ideal system, and silica sand (David Ball Group PLC and Marchington Stone Ltd), to represent natural sediment. Homogeneous and heterogeneous configurations of these materials were developed, the latter having a layered contrast between high- and low-K media. High-K and low-K material was produced for both glass beads and natural sediment (Table 1). High- and low-K material have respectively large and small grain sizes, with extra kaolin clay (Speswhite, Imerys Performance Materials Ltd) added to the low-K material to further reduce the K value. These are similar to the materials used in experimental work described in Gill et al. [9]. Further information on material properties and the consolidation method used for homogeneous experiments is in the supporting information (Sections S.1.1 and S.1.2 respectively). The layered K contrast was achieved by first wet packing the low-K material into the test cell until the compacted material filled half the chamber. The surface of the low-K material was smoothed with a metal spatula and the loose high-K material added above and consolidated using the shaker Table method (see supporting information, Section S.1.2). After the addition of high- and low-K material the chamber lid was secured before saturation of the media with synthetic groundwater.

A synthetic groundwater was used to simulate an electrical conductivity of 700 $\mu S\,cm^{-1}$, based on natural groundwater sampled in a UK aquifer [12]. This was achieved using a NaCl-deionised water solution (0.3 g-NaCl L^{-1}), prepared with deionised water sterilised by tangential flow filtration unit (1 μm filter). The test cells containing the consolidated material were saturated with synthetic groundwater from the base up at a low flow rate to remove entrapped air and then sealed.

2.2. Bench-scale setup

An experimental test cell was developed for the preparation of reproducible sections of packed materials with high- and low-K (Fig. 1). This is the same test cell used in Gill et al. [9], further details are in the supporting information, Section S.1.3.

After consolidation and enclosure of material in the test cell synthetic groundwater and the amendment solution was circulated at 10 mL min^{-1} from the reservoir tank into the cathode chamber using a peristaltic pump (Ismatec, REGLO MS-4/8). This was done until the fluid in the cathode chamber had been displaced to waste (approx. 3.5 h). A baseline sample of the pore fluid (using ports along the cell side) was taken before direct current was applied to the system from a power pack (Digimess, PM6003-3).

Samples of pore fluid for chemical analysis were taken every 2 days during the experiment, with the exception of a 4-day break between the 5th and 6th sampling time points (at days 10 and 14). Within the sediment chamber, eight narrow bore (ID = 0.5 mm) PEEK tubes were distributed in two rows of four, one for each of the high and low-K layers, with an extra sampling tube in each electrode chamber. Sampling tubes were placed inside the sediment chamber prior to consolidation and material packed around them. Blockages were prevented by fitting a small ($5 \times 10 \times 20$ mm) cube of porous sintered glass to the end of each tube. Each pore fluid sample was 1 mL to ensure minimal disturbance. Ten voltage probes consisting of 4 mm diameter 316 stainless steel rods housed in HDPE piping and distributed in two rows of five, one for each of the high and low-K layers. Voltage

Table 1
Properties of material used in experiments.

Material		Porosity, n (–)	K ($m\,s^{-1}$)	Grain Diameter (mm)	Relative composition (%)
Glass Beads	High-K	0.30	9.2×10^{-4} ($\pm 8.8 \times 10^{-5}$)	1.4	100
	Low-K	0.34	5.7×10^{-7} ($\pm 2.4 \times 10^{-7}$)	0.25	80
				0.50	10
				Kaolin	10
Silica Sand	High-K	0.39	7.0×10^{-4} ($\pm 4.9 \times 10^{-5}$)	2.4–1.2	100
	Low-K	0.44	5.9×10^{-7} ($\pm 2.8 \times 10^{-8}$)	<0.15	90
				Kaolin	10

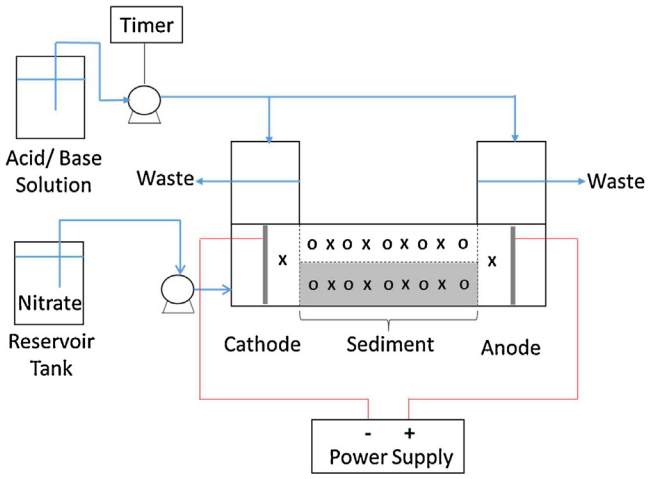

Fig. 1. Schematic of test cell design (volume 7.5 L), showing sediment chamber containing high and low-K zones (light and dark shades respectively), voltage probes (O) and sampling ports (X). Electrode chambers (each 2 L), power supply, pH control and amendment delivery mechanisms are included.

and electric current was logged every 24 h during tests using a multimeter (Digitek, DT-4000ZC). All heterogeneous experiments included two layers of sampling ports, although the majority of the homogeneous media tests used a single layer of sampling ports in the centre of the test cell.

Nitrate was selected as it is a representative ionic amendment used extensively in electrokinetic-bioremediation studies [4]. Bromide was used as a conservative tracer in control experiments under an electric field as it has similar electromigration transport properties to nitrate. Amendments were added to the cathode at a rate of 1.5 mL min^{-1} from a 10 L reservoir tank maintained at a constant concentration of either nitrate or bromide solutions. The reservoir tank was topped up at regular intervals.

2.3. Analytical methods

Samples of pore fluid were analysed for major ions (nitrate, chloride, bromide, sulphate, sodium and potassium) and pH and electrical conductivity using ion selective electrodes and standard methods. More detail on the analytical method for the major ions analysis is in the supporting information, Section S.1.4.

2.4. Electrokinetic apparatus and test conditions

A direct current was applied at a constant current strength of 25 mA (1.6 A m^{-2}) to allow more effective control of pH changes at the electrodes. A peristaltic pump (Ismatec, Ecoline VC-MS/CA 8–6) was used to circulate acid and base solutions (1 M HCl and NaOH) to the cathode and anode, respectively, to neutralise electrolysis reactions as follows:

$$\text{Anode}: \quad 2H_2O - 4e^- \rightarrow 4H^+ + O_2 \tag{1}$$

$$\text{Cathode}: \quad 4H_2O + 4e^- \rightarrow 4OH^- + 2H_2 \tag{2}$$

The rate of acid (H^+) and base (OH^-) generation can be estimated, assuming steady-state electrolysis and 100% Faradaic efficiency at the electrode [13]:

$$R_{H^+} = \frac{I}{F} \tag{3}$$

where R_{H^+} is the rate of H^+ (or OH^-) generated (mol s^{-1}). These values were used to determine the volume of acid or base required to neutralise electrolysis reactions, dosing being controlled by a timer and applied every 3 h. The pH of the electrode chambers was checked every two days by removing a 1 mL aliquot and manually titrating it to pH 7 if required. Furthermore, applying a constant current creates a fluctuation in the voltage gradient which subsequently effects the rate of electrokinetic transport processes. This can be accounted for by normalising mass transport processes to the voltage between electrodes. Details on electrode properties are in the supporting information, Section S.1.5. In experiments where electroosmotic flow was evident a Mariotte bottle was used to ensure that the anode compartment was not depleted of water and no hydraulic gradient developed. This was only relevant in homogeneous systems because any fluid transport by electroosmosis in heterogeneous systems could be countered by fluid flow through the high-K section.

2.5. Testing program

The details of all experiments run are shown in Table 2. Heterogeneous experiments comprised two layers of high- and low-K glass bead/kaolin mixes, one run without nitrate (HET_1) and three with different starting concentrations (0.1, 1 and 5 g-NO_3^- L^{-1}, HET_2-4, respectively). Homogeneous experiments

Table 2
Design of nitrate migration and control experiments.

Name	EK Properties		Reservoir Tank Properties		Sediment Properties		Reps
	Current applied	Current (mA)	Ion	Conc (g L^{-1})	Type	Configuration	
HOM_1	Yes	25	–	–	GB	HOM (Low-K)	1
HOM_2	Yes	25	NO_3^-	0.1	GB	HOM (Low-K)	1
HOM_3	Yes	25	NO_3^-	1	GB	HOM (Low-K)	2
HOM_4	Yes	25	NO_3^-	5	GB	HOM (Low-K)	1
NS-HOM_5	Yes	25	NO_3^-	1	NS	HOM (Low-K)	1
HET_1	Yes	25	–	–	GB	HET	1
HET_2	Yes	25	NO_3^-	0.1	GB	HET	1
HET_3	Yes	25	NO_3^-	1	GB	HET	2
HET_4	Yes	25	NO_3^-	5	GB	HET	1
NS-HET_5	Yes	25	NO_3^-	1	NS	HET	1
C-HOM_1	Yes	25	Br^-	1	GB	HOM (High-K)	1
C-HOM_2	Yes	25	Br^-	1	GB	HOM (Low-K)	1
C-HOM_3	No	–	Br^-	1	GB	HOM (High-K)	1
C-HET_1	No	–	Br^-	1	GB	HET	1

consisted of the same low-K material used in heterogeneous experiments, with one containing no nitrate (HOM_1) and three with different starting concentrations (0.1, 1 and 5 g-NO_3^- L^{-1}, HOM_2-4, respectively). Furthermore, both homogeneous and heterogeneous scenarios were run using natural sediment with a nitrate concentration of 1 g-NO_3 L^{-1} (NS-HOM_5 and NS-HET_5, respectively). Two types of control experiments using bromide were run, in which (1) no electric field was applied, to isolate the influence of extracting fluid from the sediment (C-HOM_3 and C-HET_1), and (2) a homogeneous system with two layers of sampling and voltage ports, to confirm that any difference between layers is not an artificial variation caused by the bench-scale setup. Replicates of homogeneous and heterogeneous systems were run for experiments at 1 g-NO_3^- L^{-1} (Table 2). All experiments were run for 336 h, except the bromide tracer experiments (192 h). The first pore fluid sample was taken 24 h after the baseline and then every 48 h to ensure minimal disturbance of the system.

3. Results and Discussion

3.1. Influence of sediment configuration on voltage gradient

3.1.1. Observed voltage difference between layers in heterogeneous and homogeneous sediments

Voltage readings taken at the same point along the sediment chamber and different heights show a greater difference in heterogeneous experiments than homogeneous experiments. This is shown in Fig. 2 where values are derived by subtracting the voltage reading of the high-K layer from the low-K layer and normalising the difference against the voltage between electrodes. Further analysis on how these values are derived from the voltage profile between electrodes is in the supporting information, Section S.2.1. The values in Fig. 2 are averages of the voltage differences observed over 10 time points after 95 h until the end of the experiment (336 h). Values are taken after 95 h to account for: (1) equilibrium with respect to nitrate mass flux into and out of the sediment chamber; and (2) the influence of nitrate migration through the sediment on the voltage difference through sediment. Further analysis is provided in supporting information, Section S.2.2. The values in Fig. 2 are normalised to the voltage between electrodes to account for the influence of applying a constant current. The influence of a variable voltage gradient between electrodes on experimental parameters and the normalisation method are discussed in the supporting information, Section S.2.3. Values for both HET_3 replicates are included in Fig. 2 (HET_3.1 and HET_3.2).

Positive and negative values in Fig. 2 indicate a higher voltage in the low- and high-K layers, respectively. Heterogeneous experiments have a predominantly positive voltage difference between layers, whereas the differences in homogeneous experiments are minimised, and either positive or negative. The heterogeneous experiment (Fig. 2A) with the highest nitrate concentration added at the cathode, HET_4, has a higher consistent voltage difference compared with other experiments. HET_3.1 shows a high peak adjacent to the anode, that is not sustained across the remaining sediment. This is in contrast to replicate HET_3.2 where the voltage difference is comparable to the remaining experiments. Homogeneous experiments (Fig. 2B) cover the range of material properties applied in this study (high-K, C-HOM_1; low-K, C-HOM_2; and low-K natural sediment, NS-HOM_5) and there is minimal difference between experiments (Fig. 2B). This implies that the properties of the heterogeneous system create this phenomenon.

3.1.2. Conceptual model of mechanisms controlling voltage differences between layers

A conceptual model for the processes in the heterogeneous experiments is presented in Fig. 3 to develop the observations in Section 3.1.1. The principal mechanism is the transfer of electrical current between layers that distorts the electric field accordingly. In order for the experimental system to replicate the conceptual model it must exhibit two specific properties: (1) the resistivity of the low-K layer must be greater than the high-K layer; and (2) a resistivity gradient must exist in the low-K layer, increasing in magnitude between the anode and cathode, that is greater than the resistivity gradient in the high-K layer. These two properties ensure that the preferential flow path for electric current is from the low- to high-K layer.

The conceptual model is based on observations made in Gill et al. [9], where a K contrast (equivalent to a spatial change in EIM) is arranged in series. The study indicated that zones of low EIM (low-K zones) corresponded to areas of low mass transport and a high voltage gradient compared with adjacent material with a high EIM (high-K zones). These observations apply to the conceptual model because the EIM is proportional to the electric current density [10], implying that current density will be higher in the high-K layer than the low-K layer (assuming a uniform distribution of ions). However, these are highly dynamic systems where the movement of electric current within a 2D setting is variable and

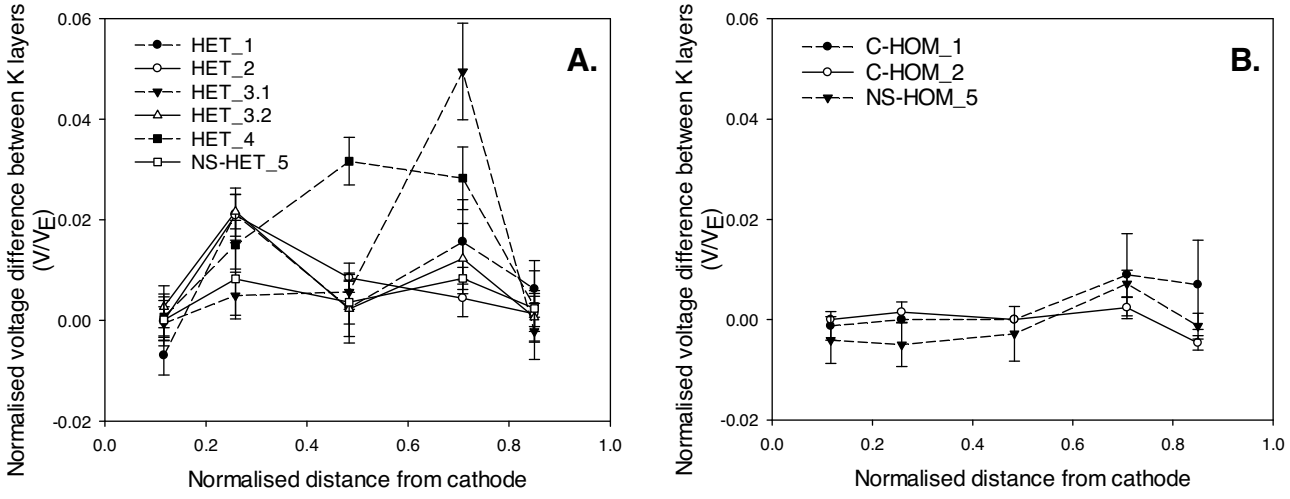

Fig. 2. Voltage difference between upper and lower sediment layers, normalised to the voltage between electrodes (V_E), against normalised distance from cathode. Graphs A and B show values from heterogeneous and homogeneous experiments, respectively. Error bars are one standard deviation from the mean.

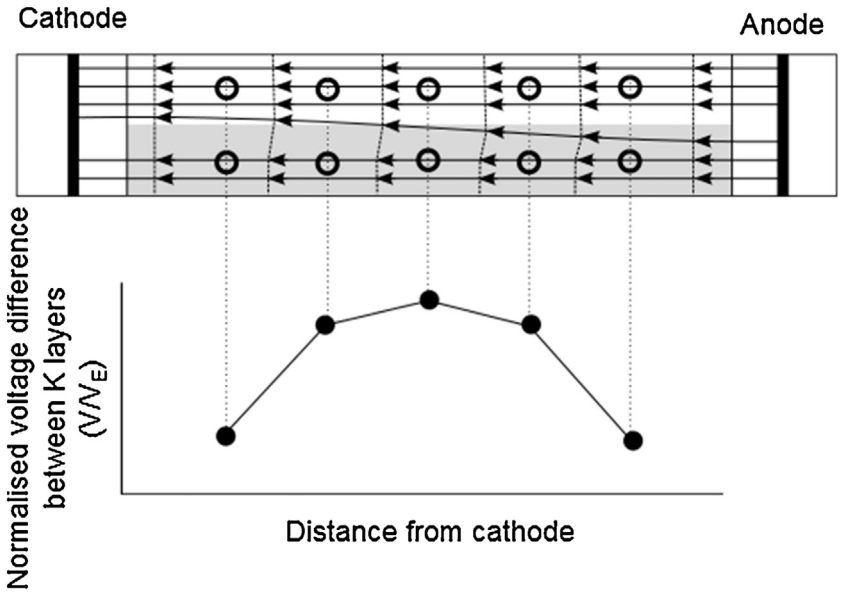

Fig. 3. Conceptual diagram showing the direction and movement of electric current (solid lines with arrow heads) through a layered heterogeneous system and subsequent effect on voltage field (dashed lines). Open circles represent the location of voltage probes; the difference between readings from high- and low-K layers is shown in closed circles below.

subject to numerous factors, with implications for the voltage difference between layers. For example, the shift in electric current depicted in Fig. 3 is fairly uniform and corresponds to a voltage difference between layers most similar to HET_4 (Fig. 2A). This contrasts with profiles from other heterogeneous experiments which indicate that current transfer is not uniform and can occur at different locations along the sediment chamber. This is represented by either a single or double peak in the voltage difference, e.g. HET_2 and HET_3.1 or HET_1, respectively (Fig. 2A).

The natural sediment experiment exhibits a small voltage difference between layers compared to the other glass bead experiments. The conceptual model suggests that this is due to minimal current transfer between layers. Certain properties of the low-K layer could create this effect. Electroosmotic flow is observed in the homogenous natural sediment experiment (see Section 3.2.1). This indicates that there is a sufficient surface charge within the low-K material to sustain electroosmotic flow. Hence, a greater proportion of the electric current could be transferred by this charge. The implication for the conceptual model is that the low-K layer of natural sediment will be more electrically conductive, minimising the movement of electric current from low to high-K layers and thus the voltage difference between layers.

3.1.3. Relationship between voltage difference and pore fluid resistivity

The effective resistivity is a property of the major ion composition of the pore fluid and is used to demonstrate how experimental observations adhere to the conceptual model outlined above (Fig. 4A–F, values for experiments HET_1 to NS-HET_5 and C-HOM_2). The parameter is derived from the effective electrical conductivity [10]:

$$\sigma^* = \sum_{i=1}^{N} F z_i u_i^* C_i \quad (4)$$

where σ^* is the effective electrical conductivity ($S\,m^{-1}$); F is the Faraday constant ($C\,mol^{-1}$); and parameters relating to ion, i: z_i is ion valence; u_i^* is the effective ionic mobility ($m^2\,V^{-1}\,s^{-1}$); and C_i, is the solute concentration ($kg\,m^{-3}$). The concentration, EIM and valency of major ions (sodium, chloride, nitrate, sulphate and potassium) in the pore fluid are used. The EIM is determined by [14]:

$$u_i^* = u_i\, n\, \tau \quad (5)$$

where u_i is the ionic mobility ($m^2\,V^{-1}\,s^{-1}$); n is porosity (−); and τ is tortuosity factor (-). Values for porosity are defined in Table 1, tortuosity values for glass beads/kaolin mix are 0.56 and 0.30 for high- and low-K material, respectively [9]. The EIM for nitrate in high- and low-K materials is 1.3×10^{-8} and $7.5 \times 10^{-9}\,m^2\,V^{-1}\,s^{-1}$; the EIM values for other major ions are in in the supporting information (Table S.1). Effective resistivity is the reciprocal of effective electrical conductivity:

$$\rho^* = \frac{1}{\sigma^*} \quad (6)$$

where ρ^* is the effective resistivity ($\Omega\,m$). The EIM for the materials in this experiment have already been characterised in a previous study [9] and observed lower values for the low-K compared to the high-K material. Therefore, based on equations (4)–(6), low-K material will have a higher effective resistivity compared to high-K material assuming uniform ion concentration.

In Fig. 4, effective resistivity is normalised to the voltage difference between electrodes. Some experiments are not included in Fig. 4 because blocked sample tubes limited sampling; these include HET_3.2, C-HOM_1 and NS_HOM_5. An ion charge balance was conducted for all experiments to confirm solute transport behaviour (see supporting information, Section S.2.5).

The conceptual model in Fig. 3 requires a higher resistivity in the low-K layer relative to the high-K layer. The smallest difference in resistivity between layers is for experiments HET_1, HET_2 and C-HOM_2 (Fig. 4A, B and F respectively). Both HET_1 and HET_2 represent experiments where no nitrate or a small amount of nitrate ($0.1\,g\text{-}NO_3\,L^{-1}$) is added at the cathode. Under these conditions there are less ions migrating into the sediment to enhance the differences between layers. Conversely in homogenous experiment C-HOM_2, $1\,g\text{-}Br\,L^{-1}$ is added at the cathode, but there is minimal difference between sample port layers across most of the sediment, except adjacent to the cathode. When compared against other heterogeneous experiments, HET_3.1 and NS-HET_5 (Fig. 4C and E respectively) with a similar $1\,g\text{-}NO_3\,L^{-1}$ nitrate addition, it is evident that the effect on resistivity is

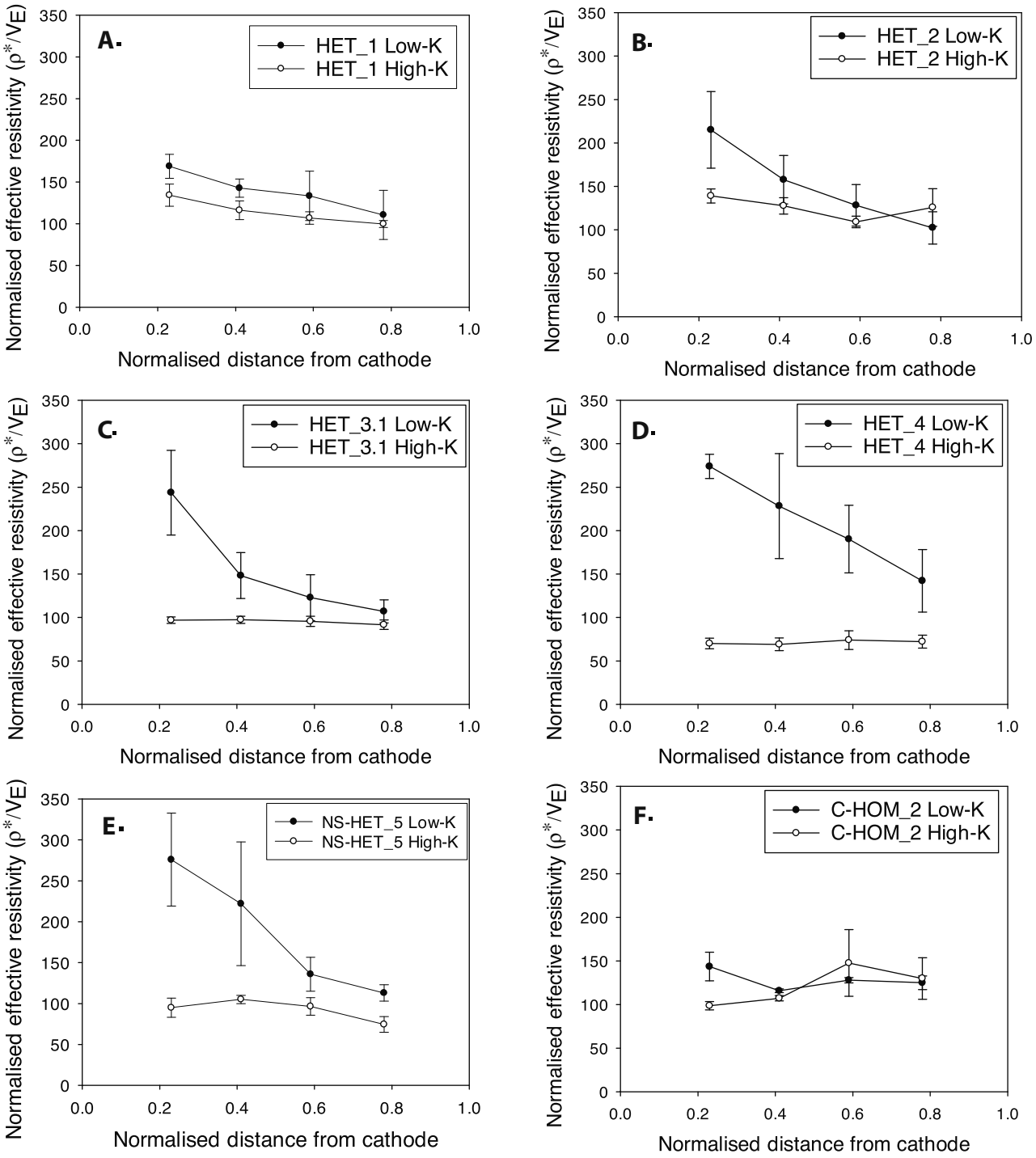

Fig. 4. Profiles of effective resistivity (ρ^*) normalised to the voltage between electrodes (V_E). Graphs represent experiments: A, HET_1; B, HET_2; C, HET_3.1; D, HET_4; E, NS-HET_5; F, C-HOM_2. Closed circles series represents data from the low-K (Tier 2 sampling ports) and open circles series represents high-K (Tier 1 sampling ports). Values are an average of 10 time points after 95 hours and error bars are one standard deviation from the mean.

minimised in the homogeneous setting. Furthermore, Fig. 4D (HET_4) shows the greatest difference in resistivity between layers, which corresponds to the highest concentration of nitrate added at the cathode (5 g-NO_3 L^{-1}).

There is evidence of a potential link between the concentration of nitrate added, subsequent scale of effective resistivity difference (Fig. 4A–E) and the voltage difference between sediment layers (Fig. 2A). Experiment HET_4 has the highest nitrate concentration and difference in effective resistivity (Fig. 4D), which corresponds to the highest consistent voltage difference (Fig. 2A). In other experiments with an increase in nitrate added at cathode and resistivity between layers (e.g. HET_1, HET_2, HET_3.1 and NS-HET_5, Fig. 4A–C and E respectively), there is no corresponding increase in the voltage difference (Fig. 2A, experiments HET_1, HET_2, HET_3.2 and NS-HET_5). However, these experiments have a voltage difference within the same range (maximum and minimum values between 0.02 to 0.005 V/V_E, respectively, Fig. 2A). This suggests that the voltage difference between layers increases as more nitrate is added at the cathode, but also that there is a threshold value at which greater differences are observed

beyond the effect of background ions. This could be linked to the proportion of the total electrical conductivity of the system, contributed by the nitrate. For example, in these experiments nitrate in HET_2, HET_3.2 and HET_4 contributed 3.4% (±0.3%) 22.6% (±1.0%) and 67.2% (±5.5%), respectively, of the total electrolyte (based on Equation (4) using ions: nitrate, chloride, sulphate, sodium and potassium).

The presence of an effective resistivity gradient increasing from anode to cathode is an important aspect of the conceptual model (Fig. 3) and is observed in all heterogeneous experiments for either the low-K or both high and low-K layers (Fig. 4). The presence of a resistivity gradient that is higher in the low-K layer than high-K layer ensures electric current travelling from the anode will shift between layers as it moves towards the cathode. If the gradient was equal or absent both the high- and low-K layers would act as resistors in parallel and no voltage gradient difference would be observed. It is difficult to elucidate a direct relationship between the observed voltage differences and resistivity gradients because additional factors could be influencing the electric field. For example, all experiments in Fig. 2A show a divergence towards the centre of the sediment section and recombine towards the electrode chambers. There is no evidence for this in the resistivity profiles, therefore the electric current could be influenced by additional factors, such as edge effects exerted by the interface between the electrode and sediment chambers. However, resistivity gradients could help explain HET_3.1 in Fig. 2A, which shows a high peak adjacent to the anode that is not observed in the replicate, HET_3.2, or equivalent natural sediment experiment, NS-HET_5. The resistivity profile for HET_3.1 in Fig. 4C clearly shows a high gradient adjacent to the cathode that is not observed to the same extent in NS-HET_5, Fig. 4D or other heterogeneous experiments. The locations of voltage difference and resistivity peak do not match, although if they are linked it would imply that a shift in electric current between layers is highly sensitive to sharp peaks in resistivity. Future experiments should consider a higher resolution of sample ports to enable more effective comparisons between the voltage difference between layers and pore fluid properties.

3.1.4. Influence of experimental parameters on voltage difference between layers

The voltage difference between layers of sediment may be sustained by the experimental setup, creating a constant rather than a transient effect. Under ideal conditions the phenomenon observed in these experiments could be assumed to dissipate once at steady-state. At this point, ion concentrations within layers would have equalised and therefore electric current would be carried proportionally through each layer and not be transferred between them to create the voltage difference. The experimental processes that could influence the voltage difference include those that increase ion concentrations within the sediment chamber over time and prevent it from reaching a steady-state. For example, the pH control system could contribute to the generation of a resistivity gradient based on an imbalance between the ion flux into the sediment at the anode and cathode boundaries. Further analysis is in the supporting information, Section S.2.6.

3.2. Transverse nitrate flux

The difference in voltage between layers is equivalent to a gradient and therefore a transverse electromigration mass flux. This is shown in Fig. 5. Nitrate migrates into the sediment from the cathode boundary. Within the sediment, the voltage difference between layers creates an associated transverse flux of nitrate. This phenomenon is demonstrated by characterising nitrate migration in homogeneous sediment and then predicting the nitrate concentration in the heterogeneous low-K layer by quantifying the flux between layers. These results relate to the second hypothesis presented in the introduction.

3.2.1. Nitrate migration through homogeneous sediment

Nitrate mass transport and velocity values through homogeneous sediment are presented in supporting information, Table S.2 in Section S.2.7. They are compared against calculated values which are derived from the method given in Section S.2.7. Good agreement between observed and calculated values indicates that nitrate migration through homogeneous materials conforms to theory. Results are also consistent with other author observations. They show that amendment mass transport increases when higher concentrations are added at the cathode [15]. The observed velocity value for the NS-HOM_5 experiments are lower than equivalent glass bead experiments due to counter electroosmotic flow in the natural sediment matrix. The electroosmotic permeability of the material was $1.2 \times 10^{-9}\,m^2\,V^{-1}\,s^{-1}$ and based on the electroosmotic pore fluid flux (see supporting information, Section S.1.6).

3.2.2. Quantifying nitrate flux between layers

The analysis of the nitrate flux between layers of sediment is split into two parts. Firstly, the observed nitrate concentration in homogeneous and heterogeneous settings are compared. Secondly, the predicted nitrate concentrations are compared.

Observed nitrate concentrations within the same material type are higher in heterogeneous experiments than homogeneous experiments, with the exception of HET_2 (Fig. 6). This difference increases as the inlet nitrate concentration at cathode chamber

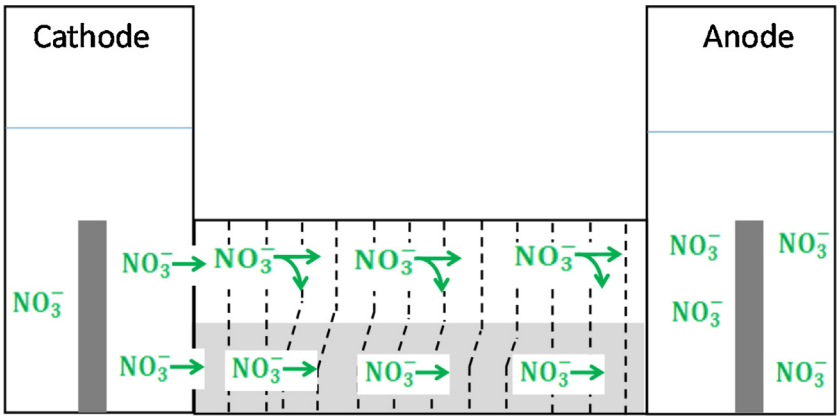

Fig. 5. Conceptual diagram showing the transverse nitrate flux within the laboratory apparatus and the distorted voltage field (dashed lines).

increases (Fig. 6A–C). Values in Fig. 6 represent the nitrate concentration across the whole sediment body at an individual time point. They are determined from pore fluid concentrations that are integrated to find the nitrate mass in the sediment; this is then divided by the pore volume, accounting for dimensions of the homogeneous or heterogeneous setting. Values are normalised to the voltage difference between electrodes. Nitrate concentrations in all experiments increase over time because the nitrate transport velocity decreases; thus nitrate residence time within the sediment increase. This is a result of applying constant current and allowing the voltage difference between electrodes to drop over time. The potential for pore fluid sampling in heterogeneous systems to artificially raise the nitrate concentration in the low-K layer is minimal compared to the mass flux into the sediment by EK (see supporting information, Section S.2.8).

A transverse mass flux between layers can be demonstrated by predicting the nitrate concentration at a particular time point; in the homogeneous setting this flux will be into the sediment from the cathode boundary, whereas in the heterogeneous setting it will be from both the cathode boundary and boundary between the high- and low-K layers. The predicted nitrate concentration in homogeneous systems is defined as the product of the mass flux into the sediment from the cathode boundary multiplied by the time before solute exits the sediment, divided by the domain volume. The time before the solute exits the system is calculated by dividing the domain length by the average velocity, v_i of ion, i ($m\,s^{-1}$), defined in these experiments as [16]:

$$v_i = \frac{u_i^* - k_e}{n} \frac{\partial E}{\partial x} \tag{7}$$

where n is the porosity of the media (−); k_e is the electroosmotic permeability ($m^2\,V^{-1}\,s^{-1}$); E is the electrical potential (V); and x is distance (m). The calculation assumes that mass flux from the cathode chamber is constant, with influx at the cathode equal to efflux at the anode. In homogeneous systems the predicted concentrations are calculated with the observed mass transport values (supporting information, Table S.2) and velocity values from a bromide tracer test conducted in similar material (high-K and low-K velocities: 6.3 and $4.4 \times 10^{-8}\,m\,s^{-1}/V\,m^{-1}$) [9].

The predicted nitrate concentration in heterogeneous systems includes an additional mass flux value to that previously defined in homogeneous conditions. This additional flux is described as a transverse mass flux and represents nitrate electromigration between the high- and low-K layers. A value for this phenomenon is obtained using the equation for 1D electromigration mass flux [14]:

$$J_i = C_i(u_i^* - k_e) \frac{\partial E}{\partial x} \tag{8}$$

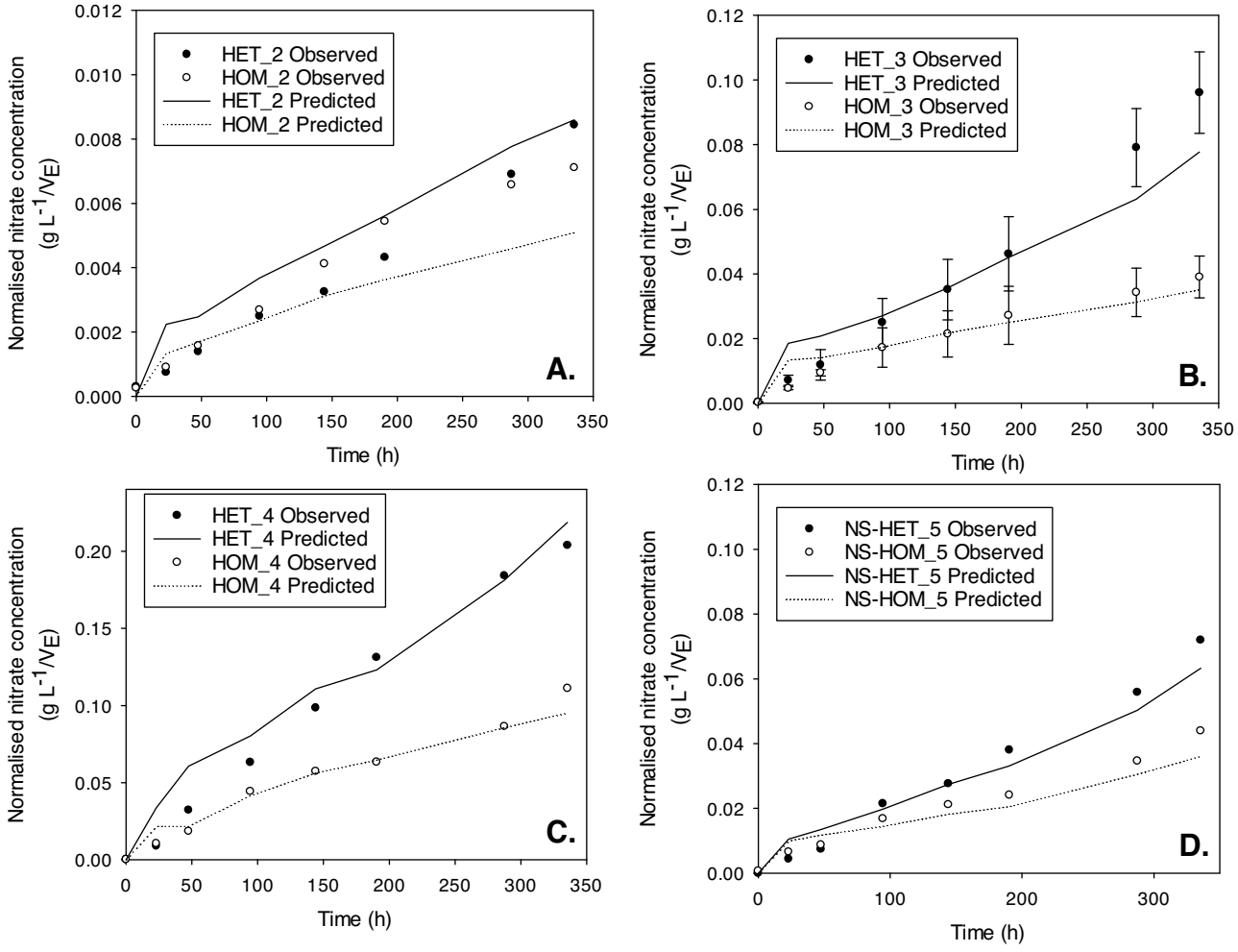

Fig. 6. Comparison of observed nitrate accumulation within the same material in heterogeneous and homogeneous settings (closed and open circles respectively) coupled with predicted nitrate concentrations (solid and dashed lines respectively). Values are normalised to the voltage between electrodes (V_E). Graphs represent experiments with nitrate added at the electrodes: A, HET_2 and HOM_2 (0.1 g-NO3 L-1); B, HET_3 and HOM_3 (1 g-NO3 L-1); C, HET_4 and HOM_4 (5 g-NO3 L-1); D, NS-HET_5 and NS-HOM_5 (1 g-NO3 L-1). Error bars represent one standard deviation from the average of values for experiments HET_3.1 and HET_3.2, and HOM_3.1 and HOM_3.2, respectively.

where J_i is the electromigration mass flux of chemical species ($kg\,m^{-2}\,s^{-1}$). Input terms for this equation, such as the nitrate concentration in the high-K layer and EIM of the material, are known. The voltage gradient between layers is the voltage difference between probe ports divided by the distance between them. To simplify the calculation, an average of voltage gradient values is taken across the length of the sediment chamber. The transverse flux is then added to the flux across the cathode boundary and incorporated into a nitrate concentration calculation for the heterogeneous setting. In Fig. 6 the predicted nitrate concentrations are shown as a solid line.

The observed and corresponding calculated nitrate concentration in heterogeneous setting are in good agreement for experiments run at 1 and 5 g-$NO_3\,L^{-1}$ (Fig. 6B–C). However, in the 0.1 g-$NO_3\,L^{-1}$ run (Fig. 6A) there appears to be little difference between the homogeneous and heterogeneous systems. This suggests that either there was minimal transverse migration of nitrate or that the effect was masked due to experimental variability. For the natural sediment experiments the difference between homogeneous and heterogeneous observed data is less than that for the equivalent glass bead experiments (Fig. 6D and B respectively). Predicted values suggest that this is due to the low voltage difference between layers. Overall, these results show that transverse electromigration is an important flux of nitrate into the low-K zone at high amendment concentrations. They are analogous to transverse or lateral diffusion observed in advection-dominated systems, where K is stratified to create high- and low-flow layers [17]. In advection-dominated systems contaminant degradation by processes such as chemical oxidation or bioremediation are limited by transverse diffusion at the high/low-K interface where solute mixing and degradation occurs [18,19]. Conversely, in EK dominated systems transverse migration is less likely to be a limiting factor. This is despite the EK transverse mass flux between layers being relatively small compared with the flux from electrodes. For example, the transverse flux between layers in HET_3 is 8.1×10^{-6} ($\pm 3.0 \times 10^{-6}$) g-NO_3 $m^{-2}\,s^{-1}$ compared with the flux of 2.7×10^{-4} ($\pm 3.1 \times 10^{-5}$) g-NO_3 $m^{-2}\,s^{-1}$ from electrodes in HOM_3. However, if the area over which the transverse flux is effective is greater than that at the electrode (such as in these experiments the electrode area is 0.0156 m^2 compared with the 0.06 m^2 area between layers) then a transverse mass flux will be an important consideration at the field scale.

3.2.3. Scalability of experimental findings

Increasing the flux of nitrate to support and enhance in situ biodegradation is crucial for effective bioremediation of organic contaminants in low-K zones, as the supply of amendment should meet or exceed the microbial capacity to ensure even distribution, [20], but is frequently limiting in these zones. Promoting the transverse flux of nitrate into low-K zones could therefore be an important factor in field applications of in situ bioremediation. A simple electron balance box model, similar to that described by Gill et al. [4], was developed to explore the importance of transverse migration observed in these experiments in an EK bioremediation scenario. To achieve an electron balance the mass transfer of electrons from electron donors (ED) (represented by organic contaminants) must equal that of electron acceptors (EA) (represented by soluble oxidants, e.g. nitrate or sulphate) for microbial respiration [21]. The model simulates the diffusion, advection and electromigration of dissolved oxygen, nitrate and sulphate (only the latter two in the case of electromigration), as well as the separate addition of nitrate as an amendment at the cathode.

The conceptual scenario created is a contaminated groundwater management issue where the goal is to prevent long-term back-diffusion of sequestered BTEX contaminants into a high-K host material. This is achieved by enhancing biodegradation of the contaminants within the low-K lens using EA delivered by different transport mechanisms. The model domain comprises a high-K host material and one low-K block (Fig. 7). The physical, chemical and electrokinetic properties of high- and low-K materials are provided in the supporting information, Section S.2.8. The model evaluated the presence and absence of a voltage gradient and transverse flux of EAs between high- and low-K materials to determine its influence on remediation timescales. Electroosmotic flow and its influence on the movement of EAs and EDs was excluded from the model.

Several scenarios are evaluated, where the mechanism controlling EA delivery varies. Scenario A, B and C represent diffusion, advection and electromigration by EK, respectively, of EAs in the surrounding groundwater to the low-K zone. In Scenario D, EK was applied and nitrate was added at the cathode (5 g-NO_3 L^{-1}). In scenario A diffusion occurs at each high-K/low-K interface, scenario B groundwater flow is directly into the low-K block, with flow direction perpendicular to the alignment of the electrodes. The numbers in Fig. 7 represent the amendment mass flux by electromigration across different boundaries. They include: (1) the nitrate flux across the cathode boundary if amendment is present; (2) the nitrate flux from the high-K host material into the low-K zone with the electric field; (3) the transverse nitrate flux from the high-K host material into the low-K zone as per the observations in these experiments; (4) the flux of nitrate out of the high-K host material; and (5) the nitrate transport time between the electrodes. The details of these calculations and their input values are in the supporting information (Table S.4–S.10). Fluxes 1–5 are relevant for scenario D, and flux 2 and 3 are relevant for scenario C. The box model assumes that EAs from the background groundwater and those added as an amendment from the cathode

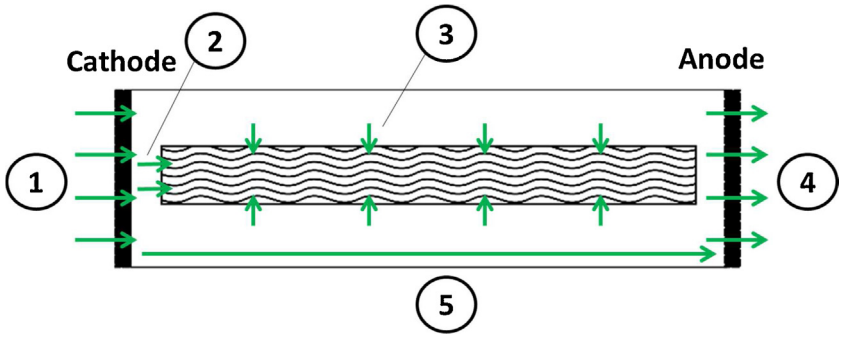

Fig. 7. Illustration of the model domain (side view) used for the conceptual analysis, showing high-K host material (white) containing a low-K block (waves). Dimensions of host material: $3 \times 1 \times 10$ m; lens: $1 \times 1 \times 9$ m. Arrows and numbers represent the different nitrate mass flux boundaries under EK.

Table 3
Results for electron balance model using four scenarios with different transport processes for nitrate amendment. Abbreviations: GW groundwater, EA electron acceptor and ED electron donor.

Scenario	Transport Mechanism	Time (years)	
		EA = ED + Transverse Flux	EA = ED − Transverse Flux
A	Diffusion	48	n/a
B	Advection	38	n/a
C	EK GW EA	2.0	2.6
D	EK NO_3^-	0.17	0.24

boundary are evenly distributed through the high-K section. In all scenarios, the background groundwater concentration of EAs is consistent due to re-supply from groundwater flow.

The results show the time required to balance the ED and EA budgets within the low-K block (Table 3). The timescales for delivery of EAs into the low-K block can be significantly reduced by the addition of EK, compared with either diffusion or advection. The presence or absence of the transverse flux had an effect on reducing the timescales. In scenarios C and D the difference was 0.6 and 0.07 years, equivalent to a time saving of 23 and 30%, respectively, over systems where a transverse flux is not developed. In scenario C the presence of a transverse flux had less effect on reducing timescales. This is due to a minimal difference in effective electrical conductivity between the high- and low-K zones compared with scenario D where nitrate is distributed at high concentration through the high-K zone (Fig. 2). Thus, this phenomenon will be more important at the field-scale when the amendment concentration introduced into the system is higher.

3.2.4. Implications for field-scale application

It is important to consider the influence of different low-K material properties on the phenomena described in these experiments. This was achieved using the conceptual model presented in Fig. 3. Low-K materials commonly encountered in the field are high-porosity clays that will exhibit both a high surface charge and a high EIM. For example, the EIM of nitrate for kaolin (representative of clays with high water content, 67% [22]) is $1.55–1.65 \times 10^{-8}\,m^2\,s^{-1}\,V^{-1}$ due to high porosity and tortuosity values [14,23]. Under these conditions the effective resistivity of the pore fluid would be lower in the low-K layer and could create a voltage difference opposite to that observed in Fig. 2. This could lead to mass flux of a negatively charged amendment from the low-K to the high-K zone. However, there are additional factors to consider at the field scale that could influence a transverse mass flux by electromigration. Firstly, the difference in resistivity between layers would need to be sufficient to initiate current transfer as per the conceptual model in Fig. 3. This is partly influenced by the contrast in EIM values. Assuming a high EIM value for a low-K material such as kaolin, a corresponding low EIM value for high-K material would be required. For example, based on the nitrate EIM contrast in these experiments and a low-K EIM of $1.65 \times 10^{-8}\,m^2\,s^{-1}\,V^{-1}$, a high-K EIM of $9.52 \times 10^{-9}\,m^2\,s^{-1}\,V^{-1}$ would be required to reproduce the voltage differences between layers observed in these experiments. Secondly, groundwater flow through the high-K layer could influence the electric current transfer in that layer. Saichek and Reddy [7] observed in a layered heterogeneous system that electric current was higher than other heterogeneous configurations due to the advective flow between the anode and cathode, facilitating electric current transport through the high-K sand layer. Thirdly, the electroosmotic permeability of materials at the field-scale may be greater than those observed in these experiments. Electroosmotic flow has been shown to generate zones of negative pressure [24]. In a layered heterogeneous systems this phenomenon could create hydraulic flow into the low-K layer and subsequently another mass flux of amendment into the low-K zone [6].

4. Conclusions

This study observes and quantifies, for the first time, a transverse flux of ions arising from voltage differences within a layered heterogeneous setting under an EK applied electric field. This is evaluated in the study using nitrate as an example ion, by considering two hypotheses. The first hypothesis predicts the presence of a voltage difference between layers of material with different effective ionic mobilities. Results show that a greater voltage difference occurs between layers within heterogeneous systems than homogeneous systems and that this difference increases with the addition of nitrate at the cathode. The conceptual model developed to explain this phenomenon links the observed voltage differences and effective resistivity values derived from pore fluid analysis.

The second hypothesis expands the concept of a voltage difference between layers, by proposing an associated mass flux of ions. This is demonstrated using a nitrate amendment and is calculated assuming parameters are known, namely the concentration of the amendment in the host material, the difference in the voltage gradient at the interface between the different materials, EIM of the different materials and surface area of the interface. Results show low-K zones within a layered heterogeneous setting relative to the flux predicted for a homogeneous setting of the same material. The importance of this process at the field-scale for an EK-BIO scenario is demonstrated using a simple electron balance model to predict biodegradation timescales in a heterogeneous setting with contaminated low-K zone for EA transport with, and without, the observed transverse flux. Overall, this flux depends significantly on the material properties, orientation of the electrodes with respect to the low-K layer and the geometry of the low-K layer itself. Future research into EK-enhanced bioremediation within heterogeneous settings should introduce both contaminant and microbial variables to observe how spatial changes in material type influence contaminant biodegradation.

Acknowledgments

The authors thank the reviewers for their insightful comments, which helped improve the manuscript. This work was completed while R.T. Gill held a UK Engineering and Physical Sciences Research Council CASE studentship with Shell Global Solutions (UK) Ltd.

Appendix A. Supplementary data

Supplementary data associated with this article can be found, in the online version, at http://dx.doi.org/10.1016/j.electacta.2016.02.191.

References

[1] US EPA, Pump-and-Treat Ground-Water Remediation: A Guide for Decision Makers and Practitioners, US EPA, Washington DC, 1996.
[2] D.A. Reynolds, B.H. Kueper, Numerical examination of the factors controlling DNAPL migration through a single fracture, Ground Water 40 (2002) 368–377, doi:http://dx.doi.org/10.1111/j.1745-6584.2002.tb02515.x.
[3] L.Y. Wick, L. Shi, H. Harms, Electro-bioremediation of hydrophobic organic soil-contaminants: A review of fundamental interactions, Electrochim. Acta 52 (2007) 3441–3448, doi:http://dx.doi.org/10.1016/j.electacta.2006.03.117.
[4] R.T. Gill, M.J. Harbottle, J.W.N. Smith, S.F. Thornton, Electrokinetic-enhanced bioremediation of organic contaminants: a review of processes and

environmental applications, Chemosphere 107 (2014) 31–42, doi:http://dx.doi.org/10.1016/j.chemosphere.2014.03.019.
[5] X. Song, E.A. Seagren, In Situ Bioremediation in Heterogeneous Porous Media: Dispersion-Limited Scenario, Environ. Sci. Technol. 42 (2008) 6131–6140, doi:http://dx.doi.org/10.1021/es0713227.
[6] A.N. Alshawabkeh, R.M. Bricka, D.B. Gent, Pilot-scale electrokinetic cleanup of lead-contaminated soils, J. Geotech. Geoenvironmental Eng. 131 (2005) 283–291, doi:http://dx.doi.org/10.1061/(ASCE) 1090-0241(2005) 131:3(283).
[7] R.E. Saichek, K.R. Reddy, Surfactant-enhanced electrokinetic remediation of polycyclic aromatic hydrocarbons in heterogeneous subsurface environments, J. Environ. Eng. Sci. 4 (2005) 327–339, doi:http://dx.doi.org/10.1139/s04-064.
[8] D.A. Reynolds, E.H. Jones, M. Gillen, I. Yusoff, D.G. Thomas, Electrokinetic migration of permanganate through low-permeability media, Ground Water. 46 (2008) 629–637, doi:http://dx.doi.org/10.1111/j.1745-6584.2008.00415.x.
[9] R.T. Gill, S.F. Thornton, M.J. Harbottle, J.W.N. Smith, Electrokinetic Migration of Nitrate Through Heterogeneous Granular Porous Media, Ground Water Monit. Remediat. 35 (2015) 46–56, doi:http://dx.doi.org/10.1111/gwmr.12107.
[10] A.N. Alshawabkeh, Y.B. Acar, Electrokinetic remediation. II: Theoretical model, J. Geotech. Eng. 122 (1996) 186–196, doi:http://dx.doi.org/10.1061/(ASCE) 0733-9410(1996) 122:3(186).
[11] B.A. Segall, C.J. Bruell, Electroosmotic Contaminant-Removal Processes, J. Environ. Eng. 118 (1992) 84–100, doi:http://dx.doi.org/10.1061/(ASCE) 0733-9372(1992) 118:1(84).
[12] S.F. Thornton, D.N. Lerner, J.H. Telham, The Technical Aspects of Controlled Waste Management: Laboratory Studies of Landfill Leachate-Triassic Sandstone Interactions, Department of Environment, London, 1995.
[13] S.S. Kim, S.J. Han, Application of an enhanced electrokinetic ion injection system to bioremediation, Water, Air Soil Pollut. 146 (2003) 365–377, doi:http://dx.doi.org/10.1023/A:1023934518049.
[14] Y.B. Acar, A.N. Alshawabkeh, Principles of electrokinetic remediation, Environ. Sci. Technol. 27 (1993) 2638–2647, doi:http://dx.doi.org/10.1021/es00049a002.
[15] S.T. Lohner, D. Katzoreck, A. Tiehm, Electromigration of microbial electron acceptors and nutrients: (I) transport in synthetic media, J. Environ. Sci. Health. A. Tox. Hazard. Subst. Environ. Eng. 43 (2008) 913–921, doi:http://dx.doi.org/10.1080/10934520801974434.
[16] M.Z. Wu, D.A. Reynolds, H. Prommer, A. Fourie, D.G. Thomas, Numerical evaluation of voltage gradient constraints on electrokinetic injection of amendments, Adv. Water Resour. 38 (2012) 60–69, doi:http://dx.doi.org/10.1016/j.advwatres.2011.11.004.
[17] L. Li, D.A. Barry, Mass transfer in soils with local stratification of hydraulic conductivity diffusion, Water Resour. Res. 30 (1994) 2891–2900.
[18] J. Hønning, M.M. Broholm, P.L. Bjerg, Role of diffusion in chemical oxidation of PCE in a dual permeability system, Environ. Sci. Technol. 41 (2007) 8426–8432, doi:http://dx.doi.org/10.1021/es0708417.
[19] J.E. Szecsody, F.J. Brockman, B.D. Wood, G.P. Streile, M.J. Truex, Transport and biodegradation of quinoline in horizontally stratified porous media, J. Contam. Hydrol. 15 (1994) 277–304, doi:http://dx.doi.org/10.1016/0169-7722(94) 90031-0.
[20] M.F. Rabbi, B. Clark, R.J. Gale, E. Ozsu-Acar, J. Pardue, A. Jackson, In situ TCE bioremediation study using electrokinetic cometabolite injection, Waste Manag. 20 (2000) 279–286, doi:http://dx.doi.org/10.1016/S0956-053X(99) 00329-3.
[21] S.F. Thornton, D.N. Lerner, S.A. Banwart, Assessing the natural attenuation of organic contaminants in aquifers using plume-scale electron and carbon balances: model development with analysis of uncertainty and parameter sensitivity, J. Contam. Hydrol. 53 (2001) 199–232, doi:http://dx.doi.org/10.1016/S0169-7722(01) 00167-X.
[22] J.K. Mitchell, Fundamentals of Soil Behavior Second Edition, John Wiley & Sons, New York, 1993.
[23] S. Thevanayagam, T. Rishindran, Injection of nutrients and TEAs in clayey soils using electrokinetics, J. Geotech. Geoenvironmental Eng. 124 (1998) 330–338, doi:http://dx.doi.org/10.1061/(ASCE) 1090-0241(1998) 124:4(330).
[24] A.N. Alshawabkeh, T.C. Sheahan, X. Wu, Coupling of electrochemical and mechanical processes in soils under DC fields, Mech. Mater. 36 (2004) 453–465, doi:http://dx.doi.org/10.1016/S0167-6636(03) 00071-1.